Medicinal Chemistry Research
https://doi.org/10.1007/s00044-020-02643-z

MEDICINAL CHEMISTRY RESEARCH

ORIGINAL RESEARCH

Dihydropyrimidones: A ligands urease recognition study and mechanistic insight through in vitro and in silico approach

Farman Ali Khan[1] · Shahbaz Shamim[2] · Nisar Ullah[3] · Muhammad Arif Lodhi[1] · Khalid Mohammed Khan[2,4] · Kanwal[2] · Farman Ali[2] · Sahib Gul Afridi[1] · Shahnaz Perveen[5] · Ajmal Khan[6]

Received: 5 July 2020 / Accepted: 23 September 2020

Abstract

Scaffold varied dihydropyrimidone derivatives **1**–**20** were evaluated for their selective urease inhibitory kinetics potential. Compounds **1**, **2**, **3**, **4**, **5**, **6**, and **12** were found to be the most promising urease inhibitors and showed the inhibition (K_i values) within the range of 9.9 ± 0.5 to 18.3 ± 0.4 μM. Lineweaver–Burk plot, Dixon plot and their secondary replots confirm that all these molecules have followed competitive mode of inhibition. Docking arrangements (MOE) revealed that all the ligands bind in the active site and therefore compete with substrate urea. Molecular docking studies of all compounds have confirmed the binding interactions of various ligands with the amino acid residues as well as Ni atoms of active site. Furthermore, these compounds **1**–**20** were also tested for their cytotoxicity against human neutrophils and plants and were found to be non-toxic.

Keywords Dihydropyrimidones · Enzyme kinetics · Michaelis–Menten kinetics · Neutrophil based cytotoxicity · Phytotoxicity

Introduction

Urease (urea amidohydrolase, EC 3.5.1.5) belongs to the family of metalloenzyme that comprises of two nickel atoms in its core structure. It catalyzes the hydrolysis of urease into NH_3 and carbamate which spontaneously hydrolyzed further and generates another molecule of ammonia along with carbon dioxide [1–4]. The speed of this reaction is approximately 10^{14} times to that of un-catalyzed reaction. In soluble form, these two molecules of ammonia and a molecule of carbonic acid are in equilibrium with their protonated and deprotonated state which results in a net increase of pH to some extent [5].

Ureases are widely distributed in nature and can be found in various plants, fungi, algae, yeasts, bacteria, some invertebrates, and in soil [6–8]. All these ureases have same common catalytic functions but different protein structures. Plants need nitrogen-containing nutrients for their growth and germination, urea is the most common fertilizer that provides essential nutrients to the plants for growth and can be easily metabolized with the action of urease enzyme that is present in plants and the microbes as well in the soil [9]. Thus, it is clear that urease plays a vital role in nitrogen metabolism of many plants as well as microorganisms [10].

Moreover, the importance of urease enzyme in plant growth and germination there are various side effects that are associated with the hyperactivity of this enzyme in agriculture. The hyperactivity of urease produces an excess amount of ammonia thus leading to environmental

✉ Muhammad Arif Lodhi
arifbiochem@hotmail.com

✉ Ajmal Khan
ajmalchemist@yahoo.com

1 Department of Biochemistry, Abdul Wali Khan University, Mardan, Khyber Pakhtunkhwa 23200, Pakistan

2 H. E. J. Research Institute of Chemistry, International Center for Chemical and Biological Sciences, University of Karachi, Karachi 75270, Pakistan

3 Chemistry Department, King Fahd University of Petroleum & Minerals, Dhahran 31261, Saudi Arabia

4 Department of Clinical Pharmacy, Institute for Research and Medical Consultations (IRMC), Imam Abdulrahman Bin Faisal University, P.O. Box 1982, Dammam 31441, Saudi Arabia

5 PCSIR Laboratories Complex, Karachi, Shahrah-e-Dr. Salimuzzaman Siddiqui, Karachi 75280, Pakistan

6 Natural and Medical Sciences Research Center, University of Nizwa, Birkat-ul-Mouz 616, Nizwa, Sultanate of Oman

Published online: 06 October 2020

problems and economical loss [8]. The high concentration of ammonia in soil at first diminishes the availability of urea as nutrient for growth of plants, secondly toxicity of ammonia affect the germination of seeds, and seedling growth thus resulting in the depriving and death of plants [11]. In order to recover the efficacy of urea and to control the economic loss, various compounds like acetohydroxamic acids, phosphoramides, and phenylphosphorodiamidate *etc* were used to inhibit the unusual hydrolysis as well as to increase the time for the absorbance of surface-applied urea into the soil [12–14].

Similarly, in the field of medicinal and veterinary sciences, urease acts as a virulent factor to produce various human pathogeneses like urolithiasis, gastric, and peptic ulcers which leads to carcinoma if left untreated [15–18]. The other pathogenic conditions associated with urease are pyelonephritis, urinary catheter encrustation, hepatic encephalopathy, and hepatic coma [8, 18–20].

Nevertheless, the most efficient approach to control the complications of urease in agriculture as well as in human beings is to discover a variety of potent and safe urease inhibitors. To date many natural products as well as synthetic compounds have been reported as possible inhibitors of urease. Many synthetic compounds like hydroxyurea, flurofamide, and hydroxamic acid have shown potential inhibition against this enzyme. However, after in vivo trials, some of these compounds have been banned due to their toxic or unstable nature; for example, acetohydroxamic acid was confirmed as teratogenic in rats [21–24]. In the same way, most of the identified inhibitors were harmful, unstable, expensive, and toxic at high concentration or may have any other side effects. Therefore, there is a direct need to design, establish, synthesize, and explore new classes of compounds against urease enzyme to identify promising candidates for drug development. Our research group had explored the synthetic dihydropyrimidone derivatives as potential urease inhibitors. All these compounds were synthesized and their in vitro urease inhibition is already reported [16]. The basic purpose of our current investigation is to study kinetics, molecular docking, and toxicities of synthetic dihydropyrimidone derivatives to gain a mechanistic insights and considerably high efficacy without any side effects in order to get rid of several health, agriculture, environmental, and economical problems.

Results and discussion

Chemistry

Dihydropyrimidone derivatives (**1**–**20**) were synthesized in one pot by reacting urea, acetylacetone and aryl aldehydes in solvent-free condition in presence of catalyst "copper nitrate trihydrate ($Cu(NO_3)_2.3H_2O$) at 80–90 °C. The targeted compounds were characterized by spectroscopic techniques like IR, EI-MS, ^{1}H-, and ^{13}C-NMR (Table 1). The detail spectroscopic data were published in our previous article [16].

Biology

Urease enzyme exists in plants, bacteria, fungi, and soil. Urease catalyzes the hydrolysis of urea to produce ammonia and carbamate ions. These carbamate ions are then decomposed to produce NH_3 and CO_2. X-ray crystallographic studies of urease enzyme have indicated the presence of two nickel (II) atoms in their active site which are bridged through oxygen. The Ni ions also showed coordination with N-atoms of imidazole, carboxylate group, and H_2O molecule [25]. The coordination mechanism of inhibitors with the active site of enzyme must be clearly understood in order to recognize the inhibition potential of these inhibitors. Since 1920, the scientists are trying to discover an accurate mechanism of action of urease but till to date it remain a matter of scientific debate [26]. During the period of 1950–1970, when the structure, mechanism and biocatalysis of enzymes were studied, jack bean urease was considered to be the most proficient, stable, and highly specific biocatalyst [26–28]. The initial mechanism of urease was proposed by Zerner and his coworkers, who suggested that one nickel atom activates the H_2O molecules while the other Ni activates the substrate urea [5]. The three dimensional study of urease active site indicates that carboxylate moiety of cysteine residue keep the urea in a stable resonance form. It has already been known that active site of urease isolated from different sources have closely related sequence of amino acids.

The synthetic molecules **1**–**20** have basic skeleton of dihydropyrimidone with variable substituents at aryl part. All these compounds have inhibited the enzyme very strongly. Kinetically, it was also identified that the ligands have shown the strength of inhibition in a concentration dependent approach. The type of inhibition was determined by Lineweaver–Burk plots, the reciprocal of the rate of the reaction was plotted against the reciprocal of substrate concentrations to monitor the effect of inhibitor on both K_m and V_{max}. Type of inhibition determines the inhibition pathway of enzyme as well as the binding moieties of inhibitors. In all these cases, V_{max} remained fixed, while K_m values were increased, which indicates that enzyme was inhibited all the time at the active site. Three different methods were applied to calculate the K_i values. First, the slope of each line in the Lineweaver–Burk plots was plotted against various concentrations of inhibitors. In a second method the K_i values were calculated when different concentrations of inhibitors were plotted against $1/K_{mapp}$, which

Table 1 Chemical structures of different dihydropyrimidone derivatives **1–20**

Compounds	R	Molecular formula	Compounds	R	Molecular formula
1	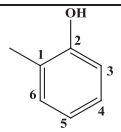	$C_{13}H_{13}N_2O_3$	**11**	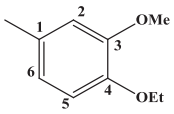	$C_{16}H_{19}N_2O_4$
2	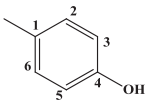	$C_{13}H_{13}N_2O_3$	**12**	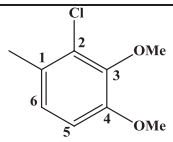	$C_{15}H_{16}ClN_2O_4$
3	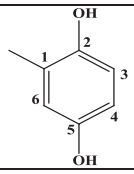	$C_{13}H_{13}N_2O_4$	**13**	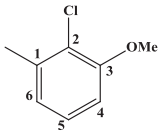	$C_{14}H_{14}ClN_2O_3$
4	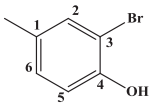	$C_{13}H_{13}BrNO_3$	**14**	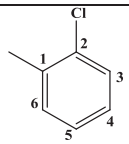	$C_{13}H_{12}ClN_2O_2$
5	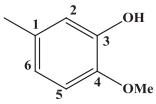	$C_{14}H_{15}N_2O_4$	**15**	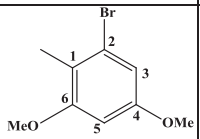	$C_{15}H_{16}BrN_2O_4$
6	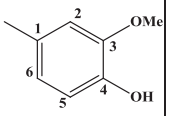	$C_{14}H_{15}N_2O_4$	**16**	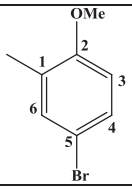	$C_{14}H_{14}BrN_2O_3$
7	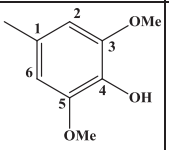	$C_{15}H_{17}N_2O_5$	**17**	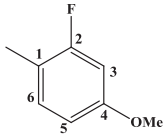	$C_{14}H_{14}FN_2O_3$
8	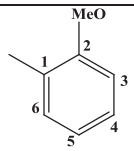	$C_{14}H_{15}N_2O_3$	**18**	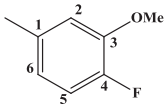	$C_{14}H_{14}FN_2O_3$
9	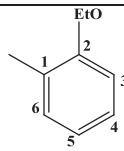	$C_{15}H_{17}N_2O_3$	**19**	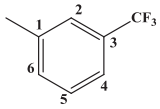	$C_{14}H_{12}F_3N_2O_2$
10	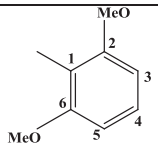	$C_{15}H_{17}N_2O_4$	**20**	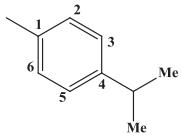	$C_{16}H_{18}N_2O_2$

Table 2 Inhibitory potential of dihydropyrimidones (**1**–**20**) against jack bean urease

Enzyme	Compounds	K_i (μM) ± SEM	K_m (mM)	K_m (mM) *app*	V_{max} (μmol/min)$^{-1}$	V_{maxapp}	Type of inhibition
Urease	**1**	12.3 ± 0.2	2.5	7.6	105	105	Competitive
	2	12.7 ± 0.7	2.5	9.0	105	106	Competitive
	3	13.4 ± 1.1	2.5	9.5	105	103	Competitive
	4	9.9 ± 0.5	2.5	6.9	105	108	Competitive
	5	11.1 ± 0.3	2.5	8.0	105	107	Competitive
	6	18.3 ± 0.4	2.5	10.7	105	102	Competitive
	7	22.2 ± 0.6	2.5	6.6	105	107	Competitive
	8	30.3 ± 0.5	2.5	8.8	105	103	Competitive
	9	24.5 ± 1.1	2.5	10.1	105	107	Competitive
	10	26.5 ± 0.1	2.5	8.4	105	104	Competitive
	11	24.2 ± 0.1	2.5	7.3	105	102	Competitive
	12	13.0 ± 0.9	2.5	9.1	105	102	Competitive
	13	11.9 ± 1.1	2.5	9.4	105	103	Competitive
	14	16.7 ± 0.4	2.5	5.9	105	107	Competitive
	15	11.2 ± 0.3	2.5	8.0	105	107	Competitive
	16	19.1 ± 0.4	2.5	10.7	105	105	Competitive
	17	14.0 ± 0.6	2.5	6.5	105	107	Competitive
	18	10.2 ± 0.5	2.5	8.9	105	103	Competitive
	19	14.0 ± 1.1	2.5	10.1	105	107	Competitive
	20	40.0 ± 0.1	2.5	9.4	105	106	Competitive

was intercept on *x*-axis. Thirdly, direct measurement of K_i values was made from Dixon plots as an intercept on *x*-axis. From the Lineweaver–Burk plots, Dixon plots along with their secondary replots, it was also confirmed that the entire series have inhibited the enzyme competitively with low K_i values (9.09 ± 0.05–40.0 ± 0.1 μM) which alternatively confirm their strength of inhibition. Furthermore, K_m, K_i, V_{max}, V_{maxapp} and K_{mapp} values of each compound along with their type of inhibition are listed in Table 2. These four types of graphs for compound **20** are presented in Fig. 1.

For structure-based drug designing, prediction of accurate protein-ligand interaction geometries were required. Thus, for this purpose molecular docking studies of all compounds (**1**–**20**) were performed, which helps to generate suitable configurations and conformations of ligands that fits well in the active site of urease and to measure their bond lengths to confirm their strength as well as to support the type of inhibition. Initially, redocking of native inhibitor (acetohydroxamic acid) was proceeded several times so as to validate the docking protocol. Then all the compounds were subjected to molecular docking to understand about the in-depth mechanism of inhibition. It was also repeated several times and lastly the best images for each compound with more interactions and less docking scores were selected for further analysis. From the docking poses, it was identified that almost all compounds showed coordination with the nickel metallocentre and some have proved as potent competitive inhibitors of jack bean urease (Table 3).

K_i (dissociation constant or inhibition constant) was determined from nonlinear regression analysis by Dixon plot and secondary Lineweaver–Burk plot at various concentrations of compounds (**1**–**20**), K_m (Michaelis–Menten constant) is equal to the reciprocal of *x*-axis intersection, V_{max} (maximal velocity) is equal to the reciprocal of *y*-axis intersection of each line for each concentration of compounds (**1**–**20**) in the Lineweaver–Burk plot. The V_{maxapp} is equal to the reciprocal of *y*-axis intersection of each line for each concentration of compounds (**1**–**20**) in Dixon plot (Each point in Lineweaver–Burk and represents the mean of three determinations).

Molecular docking plays a key role in drug designing by providing the binding mechanism of ligands with their target proteins. In the present study, molecular docking of synthetic analogs **1**–**20** was performed by using MOE 2009–2010 software. It has been proved that some of the compounds adjusted well in the active pocket of enzyme by making strong interactions with specific amino acid residues and Ni ions. Docking results of most active compounds have been discussed (Table 3).

Compound **1** has inhibited the urease very strongly by adjusting itself in the active pocket through four strong interactions with different amino acid residues. His323 has made a very strong acidic interaction with the carbonyl oxygen of pyrimidone moiety showing bond length of 1.74 Å. Kcx220 and His222 have given a couple of polar interactions with the hydrogen of hydroxy group in the

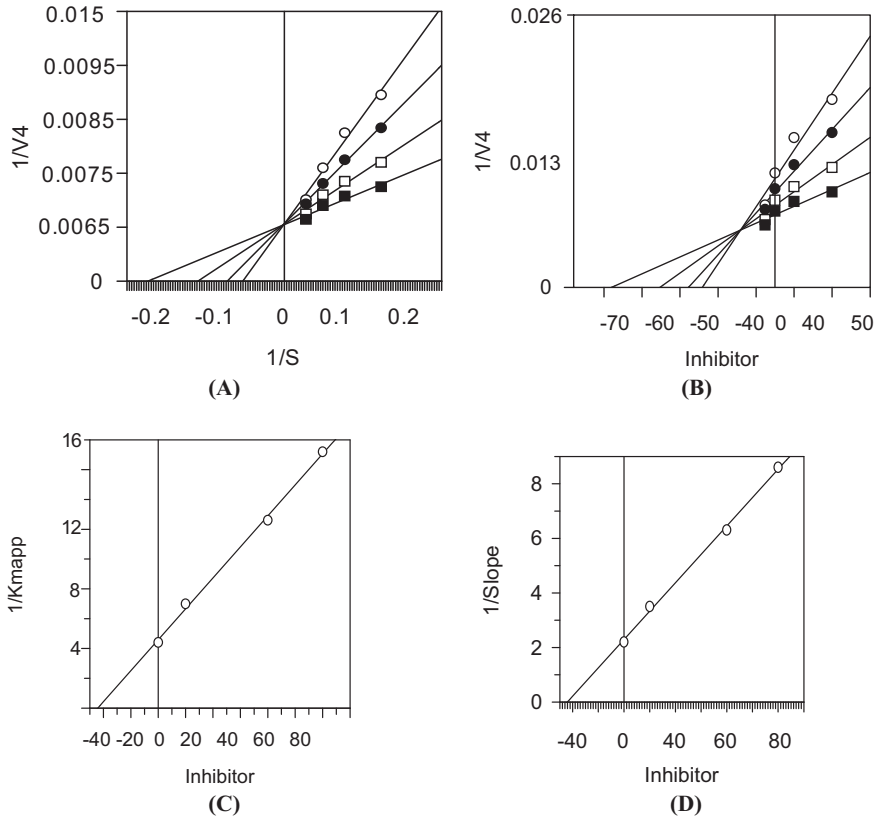

Fig. 1 Steady-state inhibition of urease by compound **20**, **A** is the Lineweaver–Burk plot of reciprocal of initial velocities versus reciprocal of four fixed Jack bean urease concentrations in absence (■) and presence of 12.5 µM (□), 25.0 µM (●), 50 µM (○) of compound **20**. **B** is the Dixon plot of reciprocal of the initial velocities versus various concentrations of compound **20** at fixed urease concentrations, (■) 50 µM, (□) 25.0 µM, (●)12.5 µM and (○) 6.2 µM. **C** is the, 1/ *Km*app versus various concentrations of compound **20**. **D**, is the, 1/*Slope versus* various concentrations of compound **20**

range of 1.79 and 3.57 Å, respectively. The last strong back bone donor interaction was shown by Ala170 with the same hydroxy hydrogen at a bond distance of 2.80 Å as shown in Fig. 2 (2D and 3D). It is also clear from the figure that Kcx220 on the other side is attached with Ni ion of active site. The second Ni ion is also present in the nearby vicinity, which greatly support the competitive type of inhibition.

Figure 3 (2D and 3D) showed that compound **2** have four different interactions with urease enzyme in three different ways. Kcx220 and Asp363 interacts through their carboxyl oxygen giving two strong polar interactions with the hydrogen of hydroxy group showing bond distances of 1.75 and 2.95 Å, respectively. On the other side, Kcx220 and His249 are in bidentate interaction with Ni ion of the active site through carboxyl oxygen of Kcx220 and imidazole ring of His249. Third interaction was observed between the hydroxyl oxygen of R group and another Ni ion at a distance of 2.84 Å which on the other side is attached with the imidazole ring of His139. The fourth very strong back bone donor interaction was given by the first NH group of pyrimidone moiety and carboxyl oxygen of Ala366 in the range of 1.88 Å.

Compound **3** interacts with the active site of enzyme through five strong interactions. A strong polar interaction was observed between the carbonyl oxygen of Kcx220 and hydroxyl hydrogen of the ligand at a distance of 1.67 Å. The carboxyl oxygen of the Kcx220 also showed interaction with the Ni ion of the active site. Subsequently, acidic interaction was shown by hydroxyl oxygen of the ligand and terminal hydrogen of Arg339 in the bond range of 2.02 Å. The remaining three strong interactions were associated with the back bone pyrimidone ring; the NH hydrogen of the skeletal pyrimidone moiety and both the hydroxy hydrogen of the R group interact with the carboxyl oxygen of the Ala366, Gly280 and Ala170, respectively. The estimated bond lengths in this case were 1.87, 2.18 and 2.50 Å, respectively, as shown in Fig. 4 (2D and 3D).

Compound **5** has inhibited the enzyme *via* four interactions of compound with different amino acid residues of the active pocket. Ala366 and Gly280 through their carboxyl oxygen atoms interact with first NH group of pyrimidone moiety and hydroxy of the ligand, respectively. The bond lengths identified in this case were 1.90 and 3.14 Å, respectively. The acidic interaction was observed between Arg339 and hydroxy oxygen of the ligand with a bond distance of 2.07 Å. The last interaction was established between the methoxy oxygen and Ni ion of the active site at a distance of 2.90 Å. The Ni ion on the other side was also involved in the interaction between the carboxyl and NH group of the imidazole ring of Kcx220 and His249, respectively, as it is clear from the Fig. 5 (2D and 3D).

Table 3 Docking score and molecular interactions of compound **1–20**

Compounds	Docking score	Ligand atom	Receptor atom	Bond type	Distance
1	−11.7450	N3	OD2-ASP 224	H-donor	3.19
		O18	O-KCX220	H-donor	2.46
		O7	NE2-HIS323	H-acceptor	2.73
2	−10.7937	N5	O-ALA 366	H-donor	2.87
		O18	O-KCX220	H-donor	2.60
3	−12.2799	N5	O-ALA366	H-donor	2.85
		O7	SG-CYS322	H-donor	3.88
		O19	O-KCX220	H-donor	2.54
		O10	NE2-HIS323	H-acceptor	3.29
4	−12.0683	N5	O-ALA366	H-donor	2.89
		O7	SG-CYS322	H-donor	3.92
		O18	O-KCX220	H-donor	2.36
		O10	NE2-HIS323	H-acceptor	3.30
5	−9.8294	N5	O-ALA 366	H-donor	2.78
		O18	SD-MET367	H-donor	3.14
6	−11.6182	O10	NE2-HIS323	H-acceptor	3.46
7	−10.3886	N5	O-ALA366	H-donor	3.35
8	−9.7147	N5	O-ALA366	H-donor	2.91
		O10	NH2-ARG339	H-acceptor	2.79
9	−10.3906	N5	O-LYS169	H-donor	3.05
		O10	NE2-HIS323	H-acceptor	2.88
10	−10.4989	N3	OD2-ASP224	H-donor	3.05
		O7	NE2-HIS323	H-acceptor	2.60
11	−10.5493	N5	O-ALA366	H-donor	2.60
		O10	NE2-HIS222	H-acceptor	3.09
12	−10.9343	N5	O-ALA366	H-donor	2.89
13	−10.3310	N5	O-ALA366	H-donor	2.90
14	−9.4726	CL18	O-ALA366	Halogen bond	2.95
15	−10.0607	O7	NE2-HIS222	H-acceptor	2.49
16	−10.3970	N3	OD2-ASP363	H-donor	3.72
		N5	O-ALA170	H-donor	2.34
		O10	NE2-HIS323	H-acceptor	3.01
17	−9.8301	N5	O-ALA366	H-donor	2.80
18	−9.4302	N5	O-ALA170	H-donor	2.68
19	−7.6193	O10	NE2-HIS324	H-acceptor	2.80
20	−10.0191	N5	O-LYS169	H-donor	3.11
		O10	NE2-HIS323	H-acceptor	2.96

Similarly, compound **6** was found to be potent inhibitor and five interactions were observed in three different ways. The hydrogen bonding interactions of ligand were observed with the NH group of imidazole ring of His139 and two carboxyl groups of Asp363 and Kcx220, respectively. The estimated bond lengths were 1.90, 2.65 and 3.08 Å, respectively. Ni also showed strong bonding interactions with the hydroxyl oxygen of compound **6** with the bond length of 2.71 Å. The second Ni of the active site showed weak interaction with the alkoxy ring of the ligand in the bond range of 4.27 Å. These interactions of both the Ni ions and amino acid residues of active site are shown in Fig. 6 (2D and 3D) which strongly supports the competitive type of inhibition.

Compound **12** also showed three different interactions. Ala366 through its carboxyl oxygen interacts with the NH hydrogen of pyrimidone moiety with bond length of 1.91 Å. A hydrogen bond interaction was observed between the Arg339 and methoxy oxygen at a distance of 2.07 Å, while the Ni ion interacts with the methoxy oxygen in the bond range of 3.00 Å. On the other hand, Ni ion was also interacting with His249 and Kcx220 which represents its

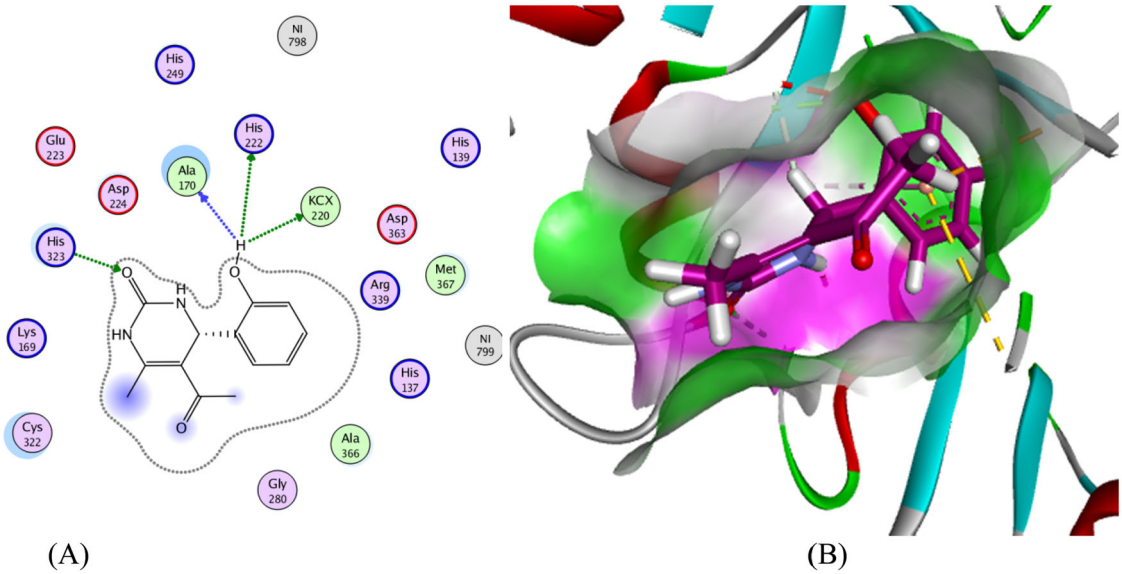

Fig. 2 Binding modes of compound **1** against jack bean urease in (**A**) 2D and (**B**) 3D

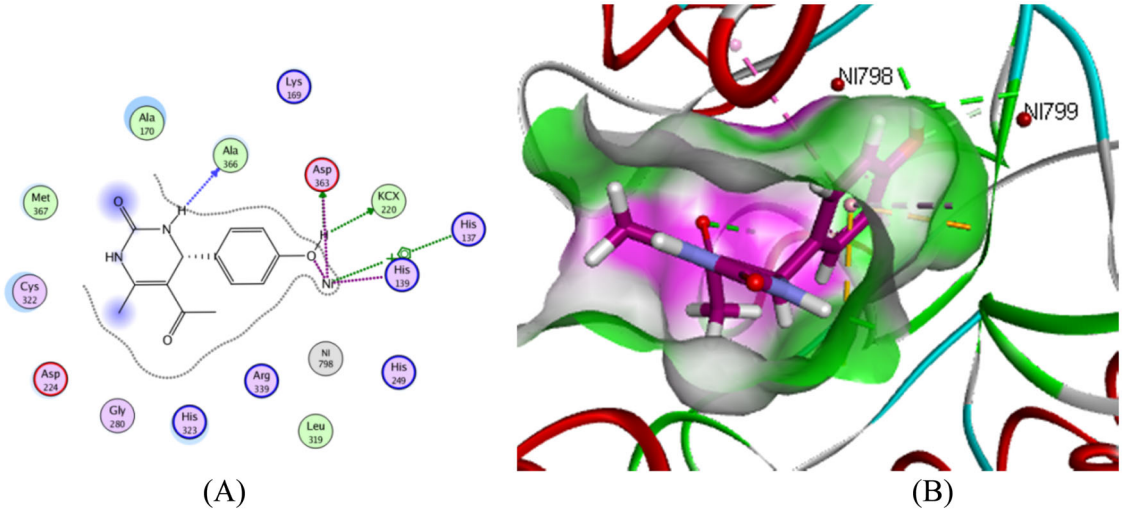

Fig. 3 Binding modes of compound **2** against jack bean urease in (**A**) 2D and (**B**) 3D

stability and active site inhibition as indicated in Fig. 7 (2D and 3D).

The toxicity effect of synthetic molecules **1**–**20** was tested against human neutrophils by using a standard operational protocol and acetohydroxamic acid was used as standard. Acetohydroxamic acid is a well-known urease inhibitor, which is most widely used to treat several urease associated diseases. The viability results of human neutrophils (1×10^7 cells per mL) against synthetic derivatives (200 µg/mL) are listed in Table 4. The results indicated that all synthetic molecules possess non-cytotoxic profile against human neutrophil cells with the exception of compound **1** which showed some toxicity against these cells.

Several classes of urease inhibitors have been discovered till now in the field of medicine as well as in agriculture. Most of them have low efficiency, various side effects on human health [6–8, 29, 30] and are also involved in causing environmental pollution [25]. This potent class of dihydropyrimidones has no phytotoxic effects on plants with the evidence of results as indicated in Table 5. They have proved to be potential therapeutic agents to treat numerous urease associated problems.

Conclusion

In the present work, we have performed the kinetics studies on 5-acetyl-6-methyl-4-aryl-3,4-dihydropyrimidin-2 (1*H*)-ones skeleton and have confirmed their competitive type of inhibition. Molecular docking and kinetics results

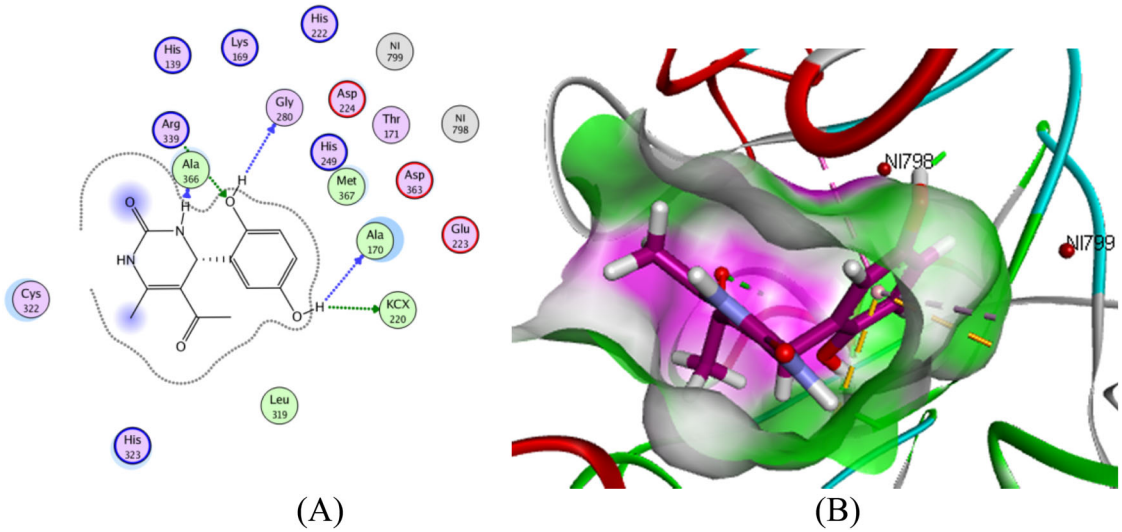

Fig. 4 Binding modes of compound **3** against jack bean urease in (**A**) 2D and (**B**) 3D

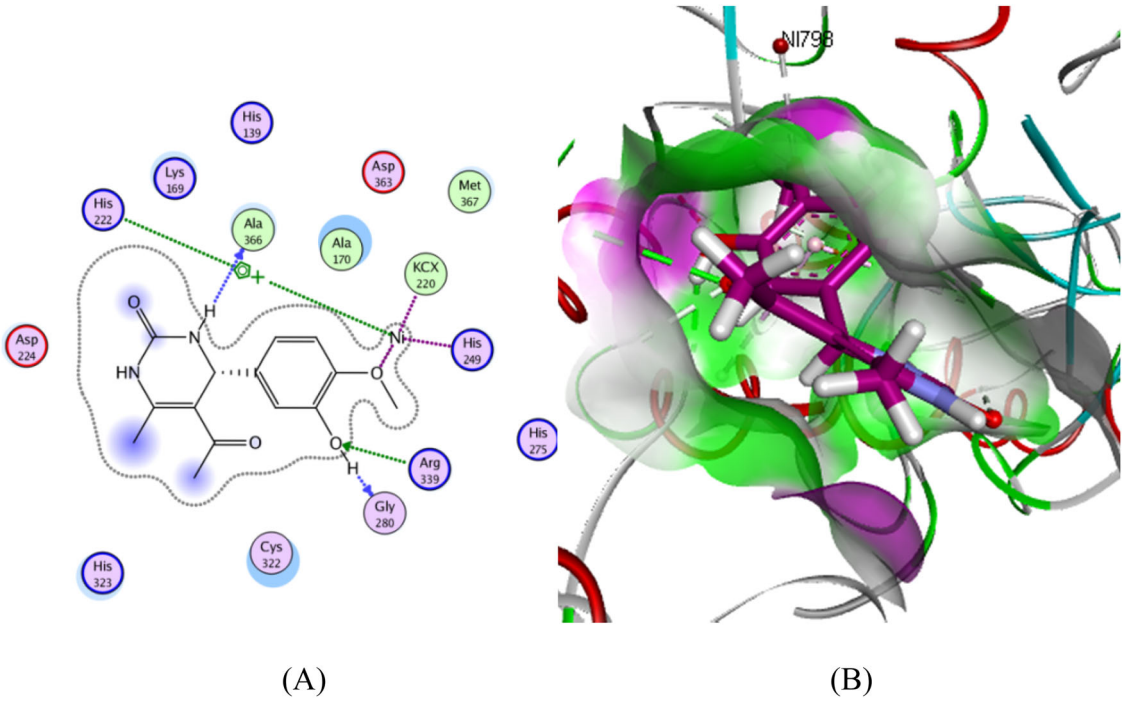

Fig. 5 Binding modes of compound **5** against jack bean urease in (**A**) 2D and (**B**) 3D

both are in line with each other. Both experiments confirm that dihydropyrimidones **1**–**20** interfere with the substrate entry into active site. Molecular docking revealed that different R groups attached with basic dihydropyrimidone is the major active pharmacophore. These compounds were also found to have nontoxic effects against human neutrophil cells and plants. From the above results it can be suggested that it is viable lead molecules for the discovery of active therapeutic agents against ureases. For future prospect, in vivo studies on animal models will further validate these results and might be helpful in developing new drug candidate.

Materials and methods

General

All the reagents and chemicals used in this study were of analytical grade. Deionized H_2O was used for the

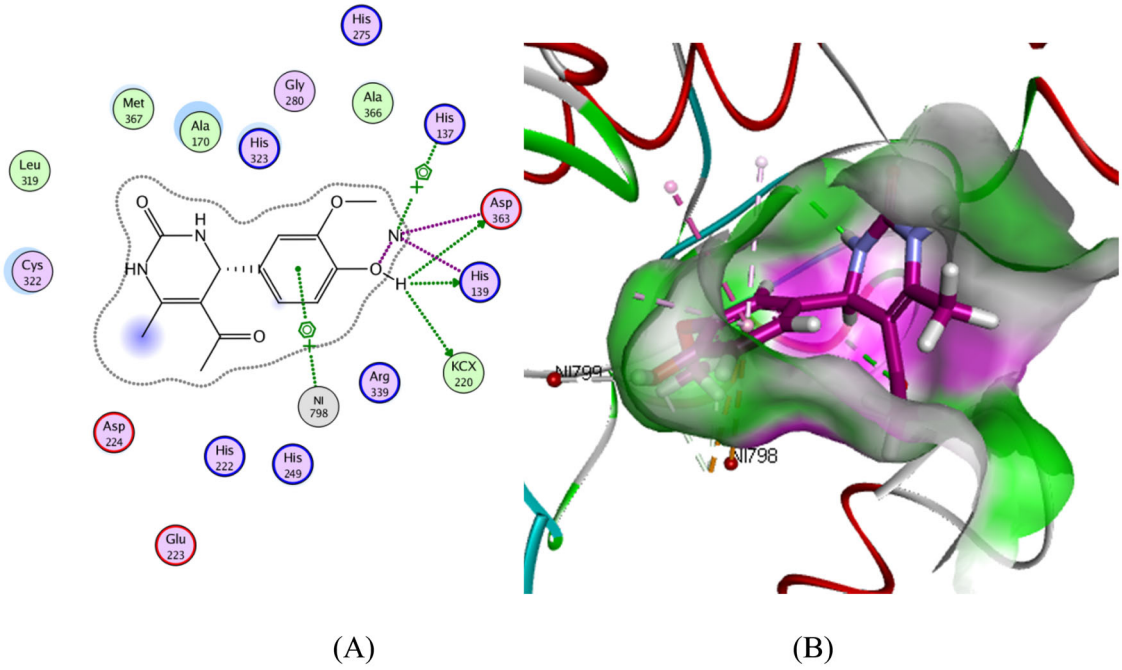

Fig. 6 Binding modes of compound **6** against jack bean urease in (**A**) 2D and (**B**) 3D

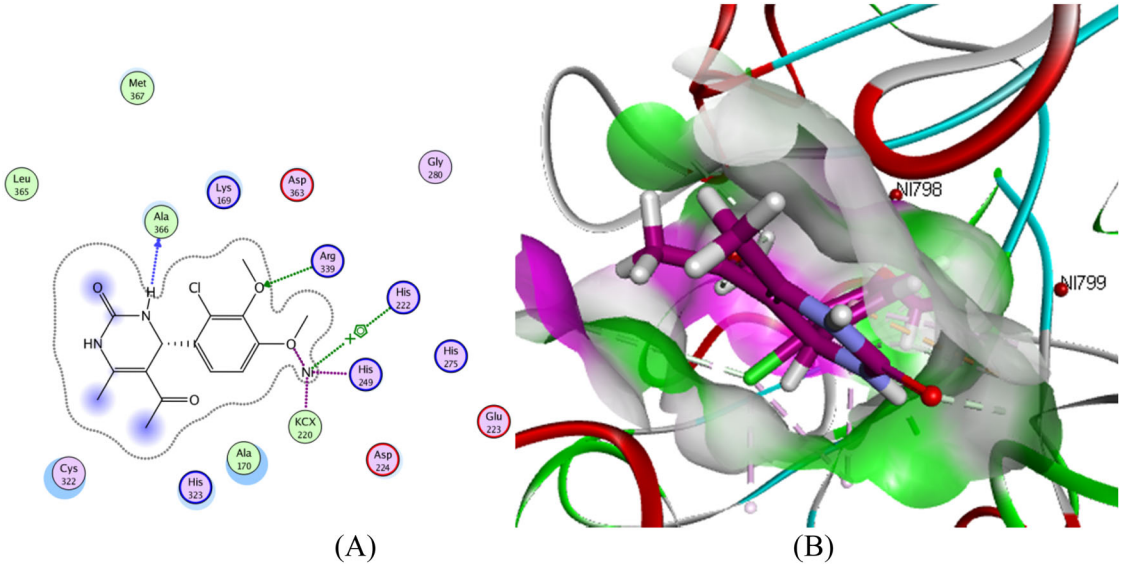

Fig. 7 Binding modes of compound **12** against jack bean urease in (**A**) 2D and (**B**) 3D

preparation of various solutions at room temperature. Type X urease (Cat. No. U4002-50 KU), urea (Cat. No. U5378), phenol (Cat. No. 16017), dipotassium hydrogen phosphate (Cat. No. 16788-57-1), DMEM-high glucose (Cat. No. D5648), and penicillin/streptomycin (Cat. No. PO781) were purchased from Sigma-Aldrich, USA. NaOCl (Cat. No. 230394M) and methanol (Cat. No. 20864.320/0823601) from BDH Lab. Supplies, UAE. Sodium hydroxide (Cat. No. S41298-4J) was purchased from Unichem, India. Thiourea (Cat. No. 1079791000) was provided by Merck, Germany. Fetal bovine serum (Cat. No. A11-104) was purchased from PAA, Austria. MTT (Cat. No. 1945921) was obtained from MP Biomedicals, France.

General procedure for the synthesis of dihydropyrimidone derivatives (1–20)

Equimolar quantities (1 mmol) of urea, acetylacetone, and aryl aldehyde derivatives were mixed and stirred at 80–90 °C. After 5 min, copper nitrate trihydrate

Table 4 Viability of human neutrophils (1×10^7 cells/mL) in the presence of compound **1–20**

Compounds	Conc. µg/mL	Viability [%]
1	200	41.16 ± 2.5
2	200	67.77 ± 3.1
3	200	80.41 ± 4.0
4	200	70.35 ± 4.2
5	200	61.28 ± 3.5
6	200	68.94 ± 4.0
7	200	66.91 ± 4.3
8	200	59.84 ± 5.2
9	200	72.0 ± 4.5
10	200	69.05 ± 4.9
11	200	56.16 ± 2.5
12	200	64.77 ± 3.6
13	200	59.01 ± 4.1
14	200	64.34 ± 4.3
15	200	64.21 ± 3.7
16	200	69.04 ± 2.0
17	200	64.01 ± 5.3
18	200	55.84 ± 3.2
19	200	52.0 ± 4.0
20	200	60.06 ± 4.2
Acetohydroxamic acid	200	88.04 ± 5.0

Mean ± SD of three experiments

Table 5 Results of *LemnaWelv*. Phytotoxicity assay

Compounds	Concentration of compounds (µg/mL)		
	1000	100	10
1	54.0	21.5	5.4
2	85.54	46.41	23.5
3	89.02	80.65	28.9
4	100	100	30.23
5	31.4	13.00	4.00
6	61.6	37.50	9.60
7	100	36.20	17.50
8	60.0	13.99	13.00
9	100	52.00	45.06
10	88.2	75.08	25.03
11	63.0	25.5	6.4
12	61.54	37.41	20.3
13	67.02	70.35	20.5
14	66.5	69.0	20.27
15	27.4	10.03	6.04
16	65.2	34.10	8.40
17	69.0	27.20	7.20
18	50.0	10.23	9.00
19	65	41.07	35.01
20	63.2	31.08	9.02
Phosphoroamide	68.9	41.3	16.0

$\{Cu(NO_3)_2.3H_2O\}$ (10 mol %) was added to the reaction mixture, in a solvent free condition. Reaction progress was monitored by TLC After completion of the reaction, the solid products were extensively washed with distilled water, hexane and recrystallized from ethanol to afford target compounds (**1–20**) (Scheme 1).

Urease inhibition assay (Indophenol's method)

Initially, 25 µL of jack bean urease solution and 5.0 µL of a test compound (0.5 mM in solvent methanol) one unit per well were taken and the mixture was incubated at 30 °C for 15 min in 96-well plate. Then 55 µL of potassium phosphate buffer (4 mM, pH 6.8) which contained urea (100 mM) was added to each well and it was again incubated at 30 °C for the next 15 min. Activity of urease was determined by the measurement of NH_3 formed through the above method as mentioned earlier by Weatherburn [31]. After that, each well of the plate was inoculated with 45 µL of phenol reagent (1% w/v phenol + 0.005% w/v Na_2-nitroprusside) and 70 µL of alkali reagents (0.5% w/v sodium hydroxide + 0.1% sodium hypochlorite). Finally, the reaction mixture was incubated third time for 50 min at 30 °C. The absorbance was measured on microplate readers at 630 nm (Molecular Devices., CA, USA) and the reactions were performed in triplicate. Thiourea was used as standard.

Analysis of the results was carried out by using the Soft Max Pro6.3 software (Molecular Device, USA). %age inhibition was measured by using the formula:

$$100 - (O.D_{\text{test well}}/O.D_{\text{control}}) \times 100$$

Determination of kinetics parameters

IC_{50} values represent inhibitory potential of compounds. Concentration of the test compounds that inhibited the hydrolysis of urea (substrate) up to 50% urea was measured by monitoring the effects of their different concentrations (from high to low) in the assay. These calculations were carried out by using the EZ-Fit Enzyme Kinetics Program *(Perrella Scientific Inc., Amherst, USA)*. ES represent the complex of Jack bean urease and urea, while P stand for the product obtained as a result of reaction. The Lineweaver–Burk plot was then applied to identify the type of inhibition, while dissociation and inhibition constants (K_i) values were calculated by applying the Dixon plots and secondary replots [32, 33]. Non-linear regression equation was applied to find out the K_m, K_i, and V_{max} values. Lineweaver–Burk plot was used for the determination of K_i

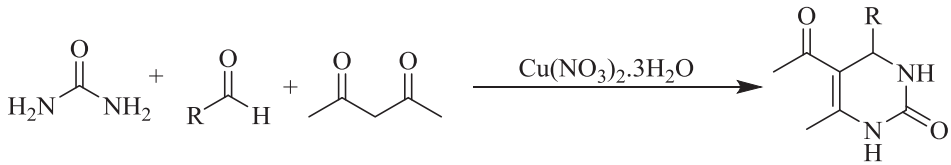

Scheme 1 General structure of synthetic compounds **1–20**

values in such a way that first at each intersection point of lines of every inhibitor concentration on *y*-axis, the values of $1/V_{maxapp}$ was calculated. In the subsequent proceeding, the slope of each line on the Lineweaver–Burk plot obtained as a result of inhibitor concentration was plotted against various concentrations of inhibitor.

Statistical analysis

Each experiment was performed in triplicate and their results were reported as a mean of three. SoftMax Pro 6.3 Software (Molecular Devices, CA, USA) was used for the analysis of these results. The graphs were plotted through GraFit program [34]. By using the same program, we have obtained the values of correlation coefficients, intercepts, slopes, and their standard errors from its linear regression analysis. The relationship for each and every line in all the graphs was more than 0.99. Each point in the graphs represents the mean of three experiments.

Molecular docking

Molecular docking was performed to determine an accurate prediction about the binding orientation of active site residues and potential inhibitors which is important for structure-based drug designing. These results were then correlated with the experimental values. Molecular Operating Environment (MOE version 2013.08) [35] docking software was used to perform such studies. Ligands as well as receptor protein (urease) preparation are the two basic steps prior to perform docking.

(a) Ligands preparation Before docking, structures of all the identified ligands were constructed through ChemDraw Ultra 12.0 (Cambridge Soft-2006, Cambridge, USA) [36], saved in the format of mol file which were then opened in MOE. Protonate 3D Option was applied for 3D protonation. The energies of identified ligands were minimized by applying the default parameters of energy minimization algorithm already adjusted in MOE (gradients: 0.05, force field: MMFF94x). Database of this series of compounds was created in mdb file format, in which all the ligands with their 3D structures were saved.

(b) Preparation of receptor protein 3D structure of urease (4UBP) having resolution of 1.55 Å, was retrieved from Protein Data Bank (PDB) [37]. Receptor protein having H_2O molecules were extracted. Like ligands, Protonate 3D Option was applied for 3D protonation. Similarly, the energy of urease protein was also minimized by applying the default parameters of energy minimization algorithm with gradients of 0.05 and force field Amber99, and then saved in pdb file format. Later on, docking of all ligands was carried out in the binding pocket of urease by following the default parameters of MOE-Dock Program. In order to increase the accuracy of protocol, re-docking was repeated [38]. After complete docking of all the ligands, the most excellent 2D as well as 3D interaction images were chosen for their specific types of interactions and to measure their bond lengths, respectively.

Cytotoxicity evaluation

The cytotoxicity of urease inhibitors **1–20** were tested against neutrophil cell lines. We used the following steps for the evaluation of cytotoxicity.

(i) Isolation of human neutrophils Heparinized fresh venous blood was taken from hale and hearty young volunteers in a City Clinical Laboratory, Dabgari Garden Peshawar, Khyber Pakhtunkhwa, Pakistan. Isolation of neutrophils was carried out through Siddiqui et al. method [39]. Accordingly, mixing of whole blood was made with Ficoll-Paque (Pharmacia Biotech Amersham, Uppsala). When sedimentation occurred, the unnecessary red blood cells (RBCs) were layered in a buffy coat way on a 3.0 mL cushion of Ficoll. Centrifugation was then carried out for 30 min at a rate of 1500 rpm. Supernatant was discarded, while pellets were collected. Furthermore, it was mixed with 0.83% of hypotonic ammonium chloride solution in order to lyse the RBCs. Again, the solution was centrifuged and Modified Hank's Solution (MHS) was used for the washing of collected neutrophils. Later on, resuspension of neutrophil cells was performed in the same solution at the rate of 1×10^7 cells per mL.

(ii) Assay procedure for neutrophil based cytotoxicity Isolated human neutrophils (1×10^7 cells per mL) were treated first with compounds under trial for 30 min and then with 0.25 mM WST-1(Dojindo Laboratories Kumamoto, Japan) on shaking water bath at 37 °C [40]. Change in absorbance was calculated at 450 nm after incubation for

3 h by using 96-well plate reader (Spectra-MAX-340, Molecular Devices, CA, USA). Here the OD represents the mean of 5 investigational replicates. Percent (%) viability of cells was measured as:

$$\%\,age\ viability\ of\ cells:$$
$$\{(OD\ test\ compound\ \times\ 100/OD\ control) - 100\} - 100.$$

Phytotoxicity evaluation

Some of the urease inhibitors are used in agriculture to reduce the pH of soil and/or to control the loss of urea. Therefore, all of the identified inhibitors were checked for their phytotoxic effects according to the modified assay of McLaughlin et al. [41]. The identified inhibitors with their three different concentrations (10, 100, and 1000 µg/mL in CH_3OH) were dissolved in sterilized E-medium. Later on, inhibitors having fixed concentrations (made by the dilution of stock solution) were taken in sterilized and clean conical flasks and allowed their evaporation for overnight. In each of the flask, 20 mL of sterilized E-medium and 10 mL *Lemna aequinocitalis* Welv plants were inoculated, already having a rosette of three fronds. For negative control only CH_3OH was added in few flasks and for positive control phosporoamide (commercially available urease inhibitors) was used. The flasks were kept in Fisons Fi-Totron 600H growth cabinet at 30 °C for a whole week having the environmental conditions (light intensity: 9000 lux, relative humidity: 56 ± 10 rh) at a short-day span of 12 h. All the experiments were performed in triplicates. Growth rate of *Lemna aequinocitalis* Welv was measured by counting the number of fronds per dose present in flasks containing inhibitors, while the growth inhibition was calculated with the reference to negative control.

Acknowledgements The authors are thankful to Higher Education Commission (HEC) Pakistan for financial support under "National Research Support Program for Universities" (Project No. 5079) and King Fahad University of Petroleum and Minerals (KFUPM) Saudi Arabia (Project No. SB191017).

Compliance with ethical standards

Conflict of interest The authors declare that they have no conflict of interest.

Publisher's note Springer Nature remains neutral with regard to jurisdictional claims in published maps and institutional affiliations.

References

1. Qin J, Zhao S-S, Liu Y-P, Man Z-W, Wang P, Wang L-N, et al. Preparations, characterization, and biological features of mononuclear Cu (II) complexes based on hydrazone ligands. Bioorg Med Chem Lett. 2016;26:4925–4929.
2. Wu C-H, Huang M-Y, Yeh C-S, Wang J-Y, Cheng T-L, Lin S-R. Overexpression of *Helicobacter pylori*–associated urease mRNAs in human gastric cancer. DNA Cell Biol. 2007;26:641–648.
3. Parsons CL. The role of a leaky epithelium and potassium in the generation of bladder symptoms in interstitial cystitis/overactive bladder, urethral syndrome, prostatitis and gynaecological chronic pelvic pain. BJU Int. 2011;107:370–375.
4. Shehzad MT, Khan A, Islam M, Halim SA, Khiat M, Anwar MU, et al. Synthesis, characterization and molecular docking of some novel hydrazonothiazolines as urease inhibitors. Bioorg Chem. 2020;94:103404.
5. Zerner B. Recent advances in the chemistry of an old enzyme, urease. Bioorg Chem. 1991;19:116–131.
6. Hausinger RP. Metabolic versatility of prokaryotes for urea decomposition. J Bacteriol. 2004;186:2520–2522.
7. Mobley H, Hausinger R. Microbial ureases: significance, regulation, and molecular characterization. Microbiol Mol Biol Rev. 1989;53:85–108.
8. Mobley H, Island MD, Hausinger RP. Molecular biology of microbial ureases. Microbiol Mol Biol Rev. 1995;59:451–480.
9. Qin Y, Cabral JM. Kinetic studies of the urease-catalyzed hydrolysis of urea in a buffer-free system. Appl Biochem Biotechnol. 1994;49:217–240.
10. Arfan M, Ali M, Ahmad H, Anis I, Khan A, Choudhary MI, et al. Urease inhibitors from *Hypericum oblongifolium* WALL. J Enzym Inhib Med Chem. 2010;25:296–299.
11. Bremner J. Recent research on problems in the use of urea as a nitrogen fertilizer. Nitrogen Econ Trop Soils. 1995;42:321–329.
12. Prakash O, Bachan Upadhyay LS. Acetohydroxamate inhibition of the activity of urease from dehusked seeds of water melon (*Citrullus vulgaris*). J Enzym Inhib Med Chem. 2004;19:381–387.
13. Rao D, Ghai S. Effect of phenylphosphorodiamidate on urea hydrolysis, ammonia volatilization and rice growth in an alkali soil. Plant Soil. 1986;94:313–320.
14. Islam M, Khan A, Shehzad MT, Hameed A, Ahmed N, Halim SA, et al. Synthesis and characterization of new thiosemicarbazones, as potent urease inhibitors: in-vitro and in-silico studies. Bioorg Chem. 2019;87:155–162.
15. Macegoniuk K, Grela E, Palus J, Rudzińska-Szostak E, Grabowiecka A, Biernat M, et al. 1, 2-Benzisoselenazol-3 (2 H)-one derivatives as a new class of bacterial urease inhibitors. J Med Chem. 2016;59:8125–8133.
16. Shamim S, Khan KM, Salar U, Ali F, Lodhi MA, Taha M, et al. 5-Acetyl-6-methyl-4-aryl-3, 4-dihydropyrimidin-2 (1H)-ones: As potent urease inhibitors; synthesis, in-vitro screening, and molecular modeling study. Bioorg Chem. 2018;76:37–52.
17. Khan I, Khan A, Halim SA, Saeed A, Mehsud S, Csuk R, et al. Exploring biological efficacy of coumarin clubbed thiazolo [3, 2–b] [1, 2, 4] triazoles as efficient inhibitors of urease: a biochemical and in silico approach. Int J Biol Macromol. 2020;142:345–354.
18. Kazmi M, Khan I, Khan A, Halim SA, Saeed A, Mehsud S, et al. Developing new hybrid scaffold for urease inhibition based on carbazole-chalcone conjugates: synthesis, assessment of therapeutic potential and computational docking analysis. Biorg. Med Chem. 2019;27:115123.
19. Khan I, Ali S, Hameed S, Rama NH, Hussain MT, Wadood A, et al. Synthesis, antioxidant activities and urease inhibition of some new 1, 2, 4-triazole and 1, 3, 4-thiadiazole derivatives. Eur J Med Chem. 2010;45:5200–5207.
20. Iqbal S, Khan A, Nazir R, Kiran S, Perveen S, Khan KM, et al. Synthesis of β-ketosulfone derivatives as new non-cytotoxic urease inhibitors in-vitro. Medicinal Chem. 2020;16:244–255.
21. Khan KM, Wadood A, Ali M, Ul-Haq Z, Lodhi MA, Khan M, et al. Identification of potent urease inhibitors via ligand-and

structure-based virtual screening and in-vitro assays. J Mol Graph Model. 2010;28:792–798.
22. Khan M, Ahad G, Manaf A, Naz R, Hussain SR, Deeba F, et al. Synthesis, in vitro urease inhibitory activity, and molecular docking studies of (perfluorophenyl) hydrazone derivatives. Med Chem Res. 2019;28:873–883.
23. Ibrar A, Kazmi M, Khan A, Halim SA, Saeed A, Mehsud S, et al. Robust therapeutic potential of carbazole-triazine hybrids as a new class of urease inhibitors: a distinctive combination of nitrogen-containing heterocycles. Bioorg Chem. 2020;95: 103479.
24. Pope AJ, Toseland N, Rushant B, Richardson S, Mcvey M, Hills J. Effect of potent urease inhibitor, fluorofamide, on Helicobacter sp. in vivo and in vitron. Dig Dis Sci. 1998;43:109–119.
25. Hawtin P, Delves H, Newell D. The demonstration of nickel in the urease of *Helicobacter pylori* by atomic absorption spectroscopy. FEMS Microbiol Lett. 1991;77:51–54.
26. Varner JE, Boyer P. Urease. The enzymes. New York, NY: Academic Press; 1960. pp. 247–256.
27. Reithel F. 1 Ureases. The enzymes: Elsevier; 1971. vol. 4, pp. 1–21.
28. Sumner JB, Somers GF. Chemistry and methods of enzymes: Academic Press Inc., Publishers, New York, NY; 1953.
29. Devesa SS, Blot WJ, Fraumeni JF Jr. Changing patterns in the incidence of esophageal and gastric carcinoma in the United States. Cancer Interdis Int J Am Cancer Soc. 1998;83:2049–2053.
30. Krogmeier MJ, McCarty GW, Bremner JM. Potential phytotoxicity associated with the use of soil urease inhibitors. Proc Natl Acad Sci. 1989;86:1110–1112.
31. Weatherburn M. Phenol-hypochlorite reaction for determination of ammonia. Anal Chem. 1967;39:971–974.
32. Lineweaver H, Burk D. The determination of enzyme dissociation constants. J Am Chem Soc. 1934;56:658–666.
33. Dixon M. The determination of enzyme inhibitor constants. Biochem J. 1953;55:170.
34. Leatherbarrow R. GraFit 5.0. Staines, UK: Erithacus Software Ltd; 1998.
35. Molecular Operating Environment Chemical Computing Group ULC. 1010 Sherbooke St West, suite 910, Montreal, QC, Canada, H3A 2R7 2018. 2018.
36. Mills N. ChemDraw Ultra 10.0 CambridgeSoft, 100 CambridgePark Drive, Cambridge, MA 02140. www.cambridgesoft.com. Commercial Price: 1910fordownload, 2150 for CD-ROM; Academic Price: 710 for download, 800 for CD-ROM, J. Am. Chem. Soc. 2006, 128, 13649-13650. ACS Publications.
37. Benini S, Rypniewski WR, Wilson KS, Miletti S, Ciurli S, Mangani S. The complex of Bacillus pasteurii urease with acetohydroxamate anion from X-ray data at 1.55 Å resolution. JBIC J Biol Inorg Chem. 2000;5:110–118.
38. Boström J, Greenwood JR, Gottfries J. Assessing the performance of OMEGA with respect to retrieving bioactive conformations. J Mol Graph Model. 2003;21:449–462.
39. Siddiqui RA, English D, Harvey K, Cui Y, Martin MI, Wentland J, et al. Phorbol ester-induced priming of superoxide generation by phosphatidic acid-stimulated neutrophils and granule-free neutrophil cytoplasts. J Leukoc Biol. 1995;58:189–195.
40. Cetin Y, Bullerman LB. Cytotoxicity of Fusarium mycotoxins to mammalian cell cultures as determined by the MTT bioassay. Food Chem Toxicol. 2005;43:755–764.
41. MacLaughin J, Chnag C, Smith D. Bench-top bioassays for the discovery of bioactive natural product: an update. Stud Nat Prod Chem. 1991;9:383–409.